Fusion Engineering and Design 138 (2019) 196–201

Contents lists available at ScienceDirect

Fusion Engineering and Design

journal homepage: www.elsevier.com/locate/fusengdes

Study on the effect of an equatorial diagnostic port plug on EM loads distribution in the CFETR blanket system

Ming Wang[a,b], Yuntao Song[a,b], Mingzhun Lei[a,*], Kun Lu[a], Sumei Liu[a], Kun Xu[a], Xianhu Zeng[a,b], Ming Li[a,b], Feng Jiang[a,b], Pengyu Wang[a,b], Shanwen Zhang[c]

[a] Institute of Plasma Physics, Chinese Academy of Sciences, Hefei, Anhui, China
[b] University of Science and Technology of China, Hefei, Anhui, China
[c] College of Mechanical Engineering Yangzhou University, Yangzhou, Jiangsu, China

ARTICLE INFO

Keywords:
CFETR
EM loads
Blanket
ANSYS
EDPP

ABSTRACT

The Chinese Fusion Engineering Test Reactor (CFETR) is the next step in China's research into fusion energy. In phase I, the preliminarily design of diagnostic systems for the CFETR was completed; however, the material and spatial position of the diagnostic systems severely affect EM loads distribution in blanket modules. In order to evaluate the effect of a diagnostic port plug on the EM loads distribution in the blanket system of CFETR, a finite element (FE) model with an equatorial diagnostic port plug (EDPP) was established using ANSYS. The EM forces and moments are calculated and discussed, followed by a comparison of EM loads in the helium-cooled ceramic breeder (HCCB) blanket to verify the EM effect of the EDPP. Simulation results show that the EM loads in the inboard (IB) and outboard (OB) blanket modules and segments were changed with the EDPP, but the direction of the main loads on the blanket system did not change. The results also show that the EDPP has a greater influence on the EM loads of the IB blanket compared to the OB blanket, meaning it is necessary to take into account the effect of the EDPP during the evaluation of the mechanical design of the blanket system in further studies. The investigation presented here may also serve as a technical reference for the design and optimization of diagnostic port plugs in the future.

1. Introduction

The China Fusion Engineering Test Reactor (CFETR) is a new superconducting magnet tokamak device, following on from the International Thermonuclear Experimental Reactor (ITER), designed for realization of fusion power by the China National Integration Design Group. One of the major scientific missions for the CFETR is to produce 200 MW (200 MW in phase I) fusion power with a tritium breeding ratio > 1 and a duty cycle time of approximately 0.3–0.5 [1]. The preliminary conceptual design of the CFETR reactor's configuration was completed by the end of 2014 and an integration engineering R&D project was started in December 2017 [2,3].

Of the in-vessel components of the CFETR, the assessment of electromagnetic (EM) loads is one of the main processes used to verify its mechanical design in detail. For the blanket system, when off-normal plasma events occur, large electromagnetic (EM) loads (of both Lorentz forces and Maxwell forces) will be inducted in each blanket module and segment [4–6]. In order to effectively evaluate the mechanical design of the blanket system, various conceptual blanket design models have been analyzed during extreme EM conditions using ANSYS code. The effect of different toroidal and poloidal segmentation of the blanket system on EM loads distribution had been studied previously by the DEMO blanket research team [7]. The structural assessments of breeding blanket systems during major plasma disruption and vertical displacement events have also been discussed in detail in previous studies [8–10]; however, the effect of a diagnostic port plug on EM loads in the blanket system have yet to be studied. The concept design of an equatorial diagnostic port plug (EDPP) in the DEMO reactor was recently reported [11] and EM and structural assessments of the EDPP performed. For the CFETR reactor, the preliminary concept design of the EDPP was completed, providing nearly 22 diagnostic techniques to provide approximately 23 measurements in phase I [12]. So far, an integration study of the blanket and the EDPP of the CFETR have not been carried out.

In order to assess the effect of EDPP on EM loads distribution in the blanket system of the CFETR, a finite element (FE) model was established using ANSYS/Emag™ software. An investigation found the worst disruption event for the component at the equatorial port is a major

* Corresponding author.
E-mail address: leimz@ipp.ac.cn (M. Lei).

https://doi.org/10.1016/j.fusengdes.2018.11.031
Received 28 August 2018; Received in revised form 19 November 2018; Accepted 21 November 2018
Available online 26 November 2018
0920-3796/

plasma disruption event; therefore, in this paper, the use of a 36 ms exponential current quench was considered [13]. The EM loads distribution on each blanket, as well as on blanket segments, were performed via the ANSYS Parametric Design Language (APDL) code. Lastly, a comparison of EM loads in the HCCB blanket was carried out to evaluate the EM effect of EDPP.

2. EDPP design description

Given that the CFETR project is in its early engineering design phase, uncertainties are inevitable regarding system requirements due to certain physical and technology issues, meaning the general guidelines for EDPP design are far from being completed. The generic concept for the EDPP was designed based on ITER's experience [14,15]. A CFETR Vacuum Vessel in a 360-degree torus is separated into 8 sectors with 45-degree each. The vacuum vessel has 4 upper ports, 8 equatorial ports and 8 lower ports. In order to meet requirements of space for the re-designing of diagnostic port plugs, and to improve the tritium breeding ratio of the CFETR, the designer adjusts the helium-cooled ceramic breeder (HCCB) blanket module distribution in the poloidal direction [6,16,17]. The updated HCCB blanket system is divided into 16 toroidal sectors of 22.5°. Each sector is then divided into 5 toroidal segments: 2 inboard (IB) segments (11.25°) and 3 outboard (OB) segments (7.5°). Poloidally, blankets 1# to 5# are defined as the IB blanket and blankets 6# to 12# are defined as the OB blanket. Fig. 1 shows a cross section of the updated HCCB blanket poloidal segmentation, with the red rectangle representing the position of the EDPP.

Fig. 2 describes the assembled EDPP which consists of three parts: the Diagnostic First Wall (DFW), Diagnostic Shield Module (DSM), and General Equatorial Port Plug (GEPP). The diagnostics will be contained within the DFW and DSM. The GEPP structure is designed as a house with four portions: (1) four thick plates (upper, bottom, left, right) and one closure plate; (2) four forged corners for jointing the four side plates; (3) a large flange designed for attaching the port plug to the CFETR vacuum vessel; (4) rails (not shown in Fig. 2) for transportation of the DSMs. The overall length of the EDPP structure (with DFWs and DSMs attached) is approximately 4.9 m, with a width of 1.7 m and a height of 2.1 m. Compared with the dimensions of ITER's port plug (L2.9 × W1.9 × H2.4 m3), it appears much longer, which may cause some technological problems such as dead-weight load effects and fixation issues, etc. [18].

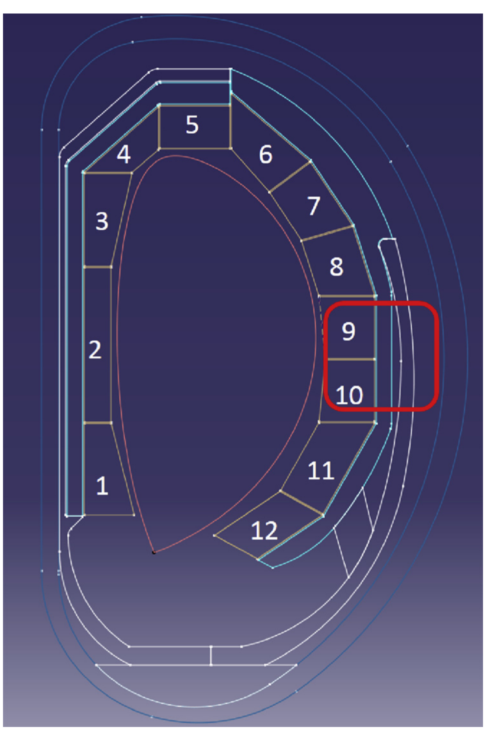

Fig. 1. Cross section of CFETR updated HCCB blanket poloidal segmentation.

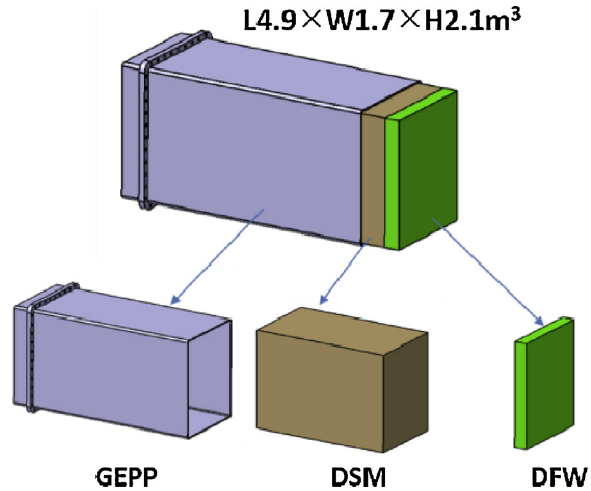

Fig. 2. Structure of assembled CFETR EDPP.

3. Finite element model

A front view of the implemented FE model developed in ANSYS is given in Fig. 3, showing the proposed 45° sector of the CFETR configuration including the blanket system, poloidal field (PF), central solenoid (CS) and toroidal field (TF) coils. For the calculations, DFW and DSM (without the GEPP structure) are simplified to a cuboid with dimensions of L4.5 × W1.5 × H1.8m^3. In order to reduce computation time, the cooling pipes in the blanket are neglected during modeling and a void fraction is used to describe the influence of the channel on resistivity [16]. The material of each component is discussed in Section 3.1.

3.1. Material properties

The materials adopted in the FE model include void, reduced activation ferritic martensitic (RAFM) steel, lithium silicate (Li4SiO4),

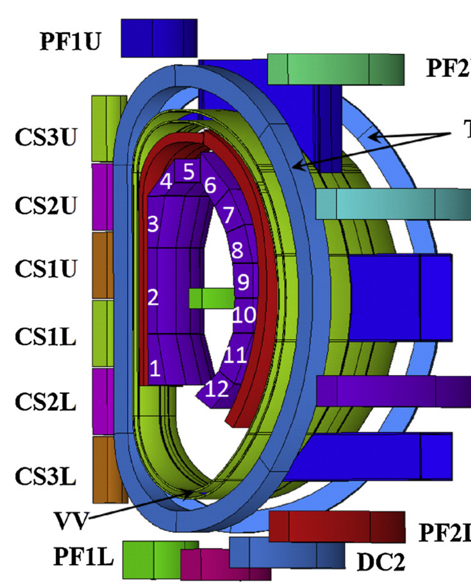

Fig. 3. The FE model of the CFETR.

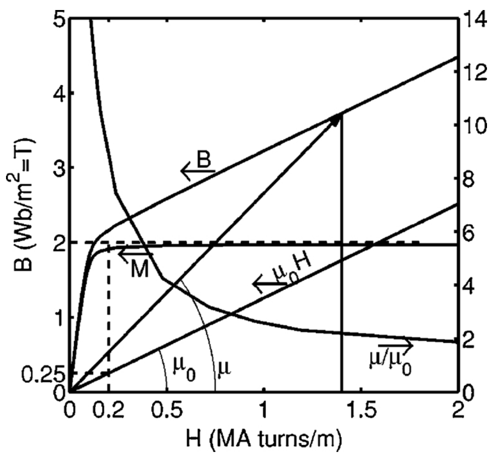

Fig. 4. B-H curve of F82H.

Table 1
Material composition and electrical properties of electrically conductive components used in the FE model.

Components	Temp. (°C)	Li_4SiO_4	316 L	EUROFE97	Avg. resistivity ($\mu\Omega$m)
VV	100		100%		0.798973
FW	320			65%	1.5303
CAP	350			70%	1.5015
BP	350			89%	1.2472
BU	325	75%		21%	1.7921
EDPP	300		100%		0.798973

beryllium (Be), and 316 L steel. The properties of RAFM steel are as F82H steel, with saturated magnetization of approximately 1.9 T; its B-H curve is shown in Fig. 4 [19]. The average temperatures are estimated for each sub-component and used in the analyses. In order to reduce computational time, the cooling pipe in the blanket is neglected during modeling and the effective resistivity was calculated according to formula (1). The material property of the updated HCCB blanket and the limit temperature are summarized in Table 1.

$$\rho_{eff} = \rho \frac{S_{eff}}{S_{\mathrm{mod}}} \tag{1}$$

3.2. Element type

For the transient analysis element type, SOLID97 and INFIN111 are used. For the void, plasma and superconducting coils, all of the KEYOPT (1) are set to zero. KEYOPT (1) = 1 is applied for the conductive components [20].

Table 2
The maximum EM forces and EM moments in the updated HCCB blanket under major plasma disruption (unit: Forces: kN; Moments: kN m).

Name	Radial		Toroidal		Poloidal	
	Force	Moment	Force	Moment	Force	Moment
IB 1	140.7	−1477.1	−20.8	180.6	122.3	−1083.3
IB 2	133.9	−1794.4	11.1	249.8	−4.3	380.6
IB 3	66.8	−1081.8	21.2	166.5	−68.2	1050.4
IB 4	−2.9	−487.3	−3.1	59.9	−32.7	168.7
IB 5	−33.3	−936.3	−25.3	79.9	−51.5	654.5
OBc6	−55.4	−579.7	−4.4	43.9	−44.1	840.3
OBc7	−54.3	−256.9	−5.9	−58.1	−35.1	823.0
OBc8	−46.5	334.1	−16.7	143.5	−21.9	759.0
OBc9	−56.9	−651.5	−34.8	222.3	54.5	328.1
OBc10	56.1	−666.1	21.9	−232.5	55.4	317.6
OBc11	54.5	−286.6	20.3	−85.2	−76.3	−1133.9
OBc12	52.1	−421.9	18.7	82.1	78.4	785
OBs6	−39.7	574.1	58.3	126.2	−32.1	852.4
OBs7	−36.1	−256.9	57.1	−55.1	−27.5	861.1
OBs8	−26.8	343.3	46.0	−161.7	−8.9	629.9
OBs9	−34.4	678.1	16.3	−279.2	23.7	342.3
OBs10	39.9	−679.6	−18.1	−288.1	22.6	−336.6
OBs11	23.4	−294.2	−66.0	113.2	−60.1	1167.6
OBs12	38.0	−400	43.0	101	25.4	367

3.3. Boundary condition

The cyclic symmetric boundary condition is used in coupling the nodes on the end of 22.5° and −22.5° of the FE model. The AX and AY degrees of freedom are set to zero to constrain the magnetic fluxes to move only in the poloidal direction. The infinite boundary condition simulates the dissipation of the EM field at infinity by adding Infinite Flags (INF). The zero potential point boundary condition uses the D command to define the VOLT degree of freedom of a node in the conductor part as zero [21].

3.4. Load

The loads of the EM analysis mainly come from the TF, PF, CS and plasma. The BFE command was used to apply the current density to the coils and plasma. In this simulation, the currents of the superconducting coils were set to a constant. As, presently, no effective plasma distribution is available for the CFETR configuration, a simple equation (formula (2)) is used to represent the plasma current quench [10].

$$I = 10^7 e^{-\tau/0.036} \tag{2}$$

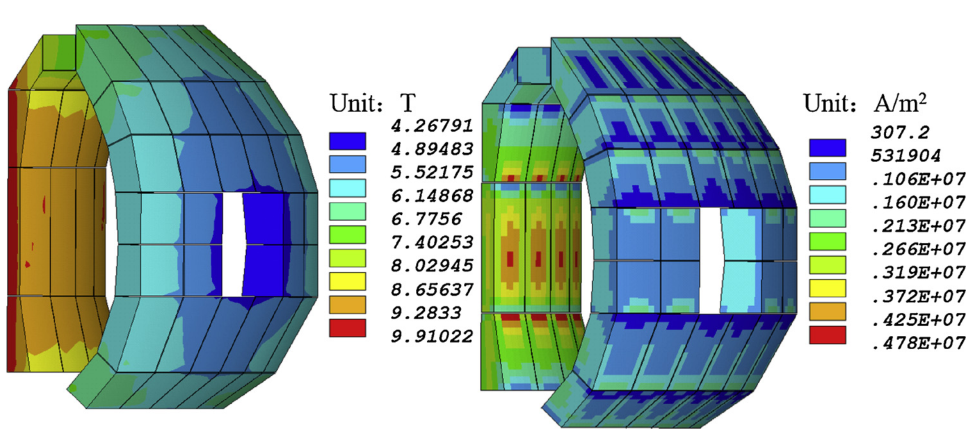

Fig. 5. The magnetic field vector and eddy current density distribution in the updated HCCB blanket (Left: the magnetic field; right: the eddy current density).

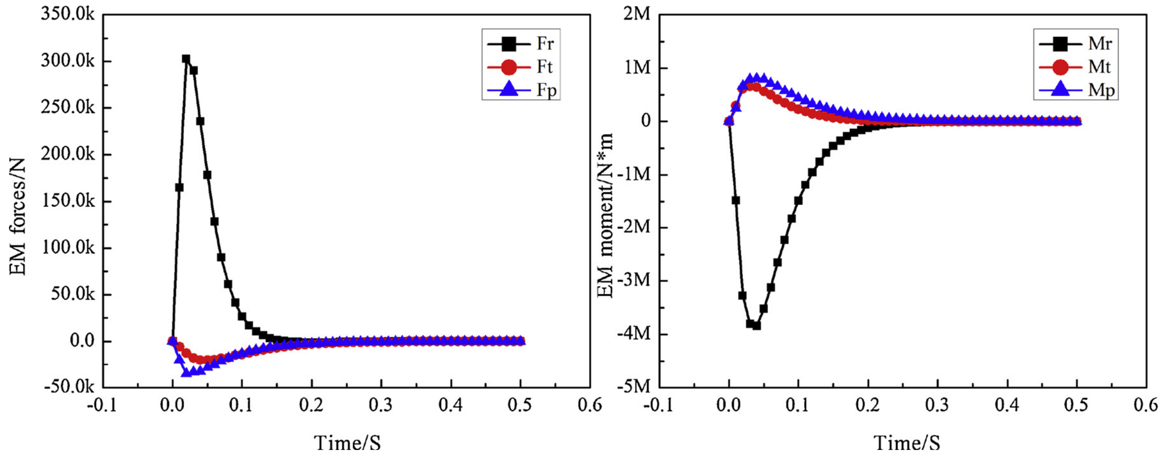

Fig. 6. Time evolution of the forces and moments for the inboard blanket.

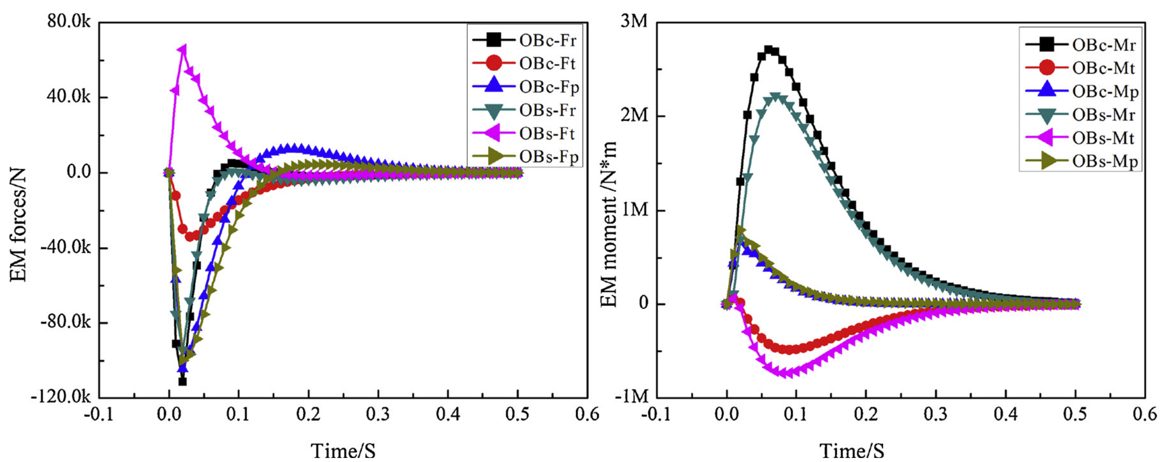

Fig. 7. Time evolution of the forces and moments for the outboard blanket.

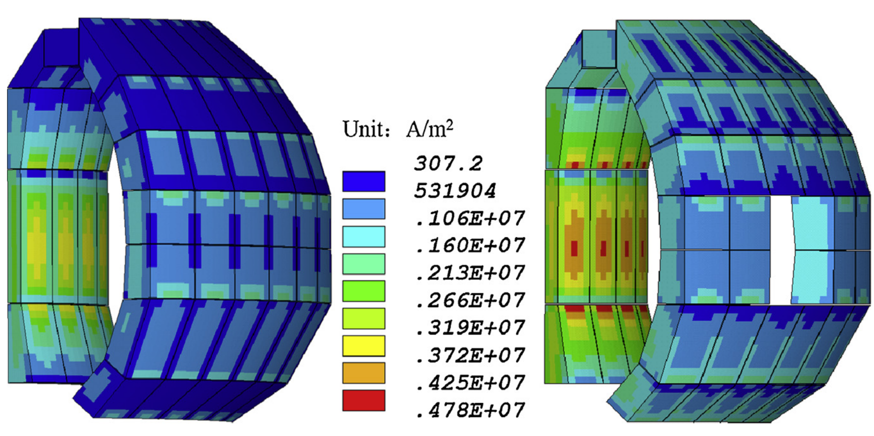

Fig. 8. The total eddy current density distribution in the updated HCCB blankets (left: updated HCCB blanket without EDPP; right: updated HCCB blanket with EDPP).

4. Results

The EM forces and moments are calculated by using FMAG and VCROSS from the internal commands of ANSYS [20]. For the moment calculation, the reference point is located in the center of the back plates of each blanket. The labels OBc and OBs are used to identify the central and side outboard blankets, respectively.

4.1. EM results of the updated HCCB blanket with EDPP

Forces distribution is calculated, along with the total force and moment acting on the blanket segment and each module. As shown in previous work, a particular eddy current loop means the total force in the blanket module is greatly reduced compared to the other directions [22]. Due to the high toroidal magnetic field in the CFETR device, the forces and moments in the radial direction are significantly larger than in the other two directions.

Fig. 5 shows the magnetic field vector and eddy current density

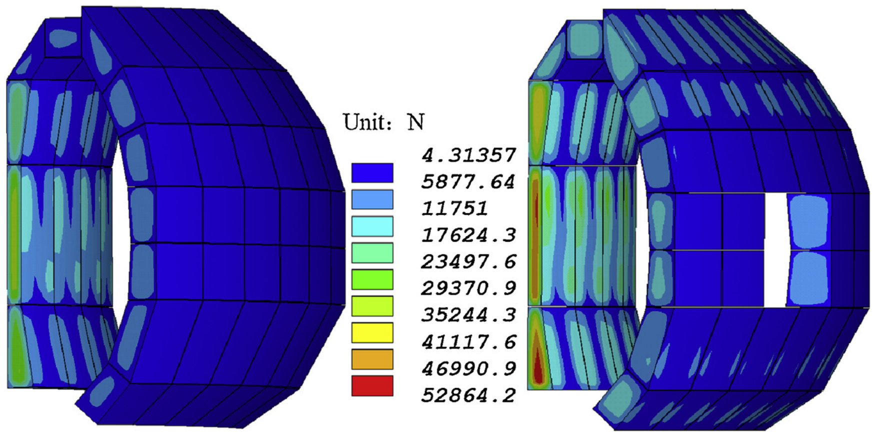

Fig. 9. Total EM forces distribution in the updated HCCB blankets (left: updated HCCB blanket without EDPP; right: updated HCCB blanket with EDPP).

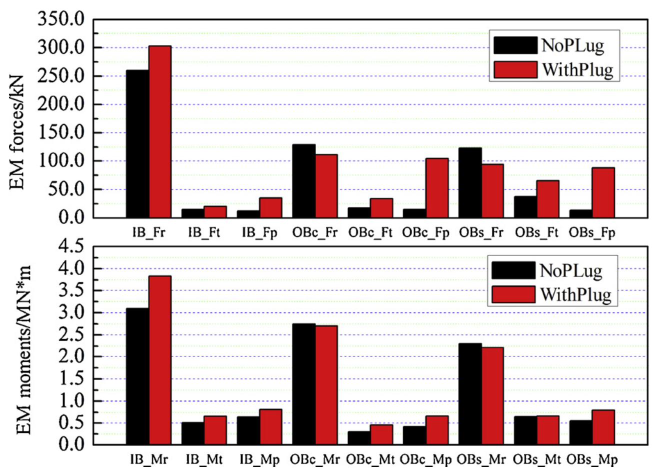

Fig. 10. Comparison of the EM forces and moments on the two FEM model (Up: EM forces; Down: EM moments).

distribution in the updated HCCB blanket. The maximum eddy current density occurs near the IB blanket and is in the order of 10^6 A/m^2. Table 2 lists the maximum EM forces and moments in each updated HCCB blanket, which includes the EDPP. The maximum EM force generated in the radial direction is 140.7 kN, and the maximum EM moment in the radial direction is 1794.4 kN m. The maximum EM force and moment loads from eddy currents induced during the major plasma disruption is on the same level as in the DEMO blanket system, although both are smaller than DEMO results; reasons for this result may include that the total plasma current of DEMO is higher than the CFETR.

Fig. 6 shows the forces and moments evaluation in the IB blanket vertical segment. Fig. 7 shows the forces and moments evaluation in the OBc and OBs blanket vertical segments, respectively. As seen in previous work, a predominant radial force and moment generated in the blanket system during the major plasma disruption occurs due to the high toroidal magnetic field (in comparison with the poloidal one). Given that both the magnetic field in the IB zone and the eddy current density are higher than that in OB zone, the maximum force and moment in the IB blanket should be higher than that in the OB blanket.

4.2. Comparison of EM loads distribution with or without EDPP

Using the current design of the CFETR blanket system, the IB and OB blanket modules will be maintained together through flexible supports and shear keys with the back plate support. In order to investigate the effect of the diagnostic port plug on the EM loads distribution in the updated HCCB blanket, a comparison is made between the eddy current and EM force distribution in the blanket system. In addition, a study of the EM loads distribution in the IB and OB blanket vertical segments is presented with respect to the FE model, with or without the EDPP.

Fig. 8 shows the total eddy current density distribution in the updated HCCB blankets, with or without the EDPP. The magnitude of the maximum eddy current density produced in both models is in the order of 10^6 A/m^2. Looking at the EDPP in the FE model, the density of eddy currents in each blanket module increase, with the maximum eddy current density in blanket#2 increasing by 57%.

Fig. 9 shows the EM forces distribution in the updated HCCB blanket. For models with or without EDPP, the maximum EM force generated is 52.8 kN and 33.0 K N, respectively. Considering the EDPP, the total EM forces in the IB blanket show a significant increase, especially for the blanket#1 and blanket#2 modules. For the OB blanket module, the distribution of the EM forces loads do not change much.

Fig. 10 shows the forces and moments comparison of the two FE models. For the IB blanket, it can be seen from the results that EM loads in the blanket vertical segment increase significantly with EDPP. For the OB blanket, forces have increased in the toroidal and poloidal direction, more so in the poloidal direction; however, after this change, the load in the poloidal direction is still smaller than in radial direction.

The EM load in the blanket module and segment have clearly changed with the EDPP, but the main loads affecting the mechanical design of the blanket system are still in the radial direction. The results show that the EDPP has a great influence on the EM loads of the IB blanket, where the maximum EM moment increases by 25%.

The DEMO research team also carried out an integration analysis of a diagnostic port plug with the blanket system, focusing on the diagnostic port plug. The team conducted an EM structure coupling analysis for the two types of diagnostic port plugs; their results show that the different sizes and orientations of the front openings in the port plug do not influence the overall behavior of the structure [12]. Based on the above analyses, future optimization of the diagnostic port plug should include small front openings, as they may reduce the effect of EM loads in the blanket system.

5. Summary

As part of ongoing CFETR design, this study focuses on the effect of an EDPP on EM loads distribution in the blanket system. A 3D model of the CFETR sector was established using ANSYS software and a major plasma disruption scenario analyzed with 36 ms exponent current quench. The eddy current density, Lorentz forces and moments were obtained for each blanket module, as well as in the segments. A comparison of the EM loads in the updated HCCB blanket was carried out to evaluate the EM effect of the EDPP.

For the updated HCCB blanket with the EDPP, the maximum values of the EM force and moment are 140.7 kN and 1794.4 kN m, respectively. Comparing the effect of the EDPP on the EM loads distribution in blanket system shows that the EM loads in the blanket module and segment have changed, but the main loads of the blanket system are still in the radial direction. The results show that the EDPP has a great influence on the EM loads of the IB blanket; therefore, in the next phase of the evaluation of the mechanical design of the updated HCCB blanket, it is necessary consider the effect of the EDPP on EM loads distribution. Moreover, the designer may adopt a diagnostic port plug with small front openings in the future, which could be useful to reduce its effect on the EM loads of the blanket system.

Acknowledgments

The author would like to express his gratitude to all the members of CFETR design team. This work is financially supported by the National Key R&D Program of China (No. 2017YFE0300604 and No. 2017YFE0300503).

References

[1] Y. Wan, Mission of CFETR, Proc. ITER Training Forum Second Workshop MFE Develop (2012) 1–6.
[2] Y.T. Song, S.T. Wu, J.G. Li, et al., Concept design of CFETR tokamak machine, Ieee Trans. Plasma Sci. 42 (3) (2014) 503–509.
[3] Y. Wan, J. Li, Y. Liu, et al., Overview of the present progress and activities on the CFETR, Nucl. Fusion 57 (10) (2017) 102009.
[4] D.H. Kim, D.K. Oh, S. Pak, et al., Eddy current induced electromagnetic loads on shield blankets during plasma disruptions in ITER: a benchmark exercise, Fusion Eng. Des. 85 (10–12) (2010) 1747–1758.
[5] R. Albanese, R. Fresa, M.F. Palumbo, et al., Electromagnetic disruption loads on ITER blanket modules, IEEE Trans. Magn. 46 (8) (2010) 2935–2938.
[6] M. Lei, Y. Song, M. Ye, et al., Conceptual design of a helium-cooled ceramic breeder blanket for CFETR, Fusion Sci. Technol. 68 (4) (2015) 772–779.
[7] I.A. Maione, A. Vaccaro, Parametric analysis of EM loads acting on DEMO vertical segments with respect to module's dimension//Fusion engineering (SOFE), 2013 IEEE 25th Symposium on. IEEE, (2013), pp. 1–6.
[8] I.A. Maione, C. Zeile, L.V. Boccaccini, et al., Evaluation of EM loads distribution on DEMO blanket segments and their effect on mechanical integrity, Fusion Eng. Des. 109 (2016) 618–623.
[9] S. Liu, P. Long, W. Wang, et al., Evaluation of electromagnetic forces on Chinese Dual Functional Lithium Lead Test Blanket Module in ITER, Fusion Eng. Des. 85 (10) (2010) 2176–2180.
[10] Ming Wang, Mingzhun Lei, Yuntao Song, et al., Electromagnetic-structural coupling analysis on CFETR helium cold ceramic breeder blanket under plasma major disruption, Nuclear Tech. 40 (6) (2017) 060601.
[11] Y. Yang, G. Li, Y. Wang, et al., Progress of concept design for CFETR diagnostic system, IEEE Trans. Plasma Sci. 46 (5) (2018) 1361–1365.
[12] G. Grossetti, L.V. Boccaccini, F. Cismondi, et al., DEMO port plug design and integration studies, Nucl. Fusion 57 (11) (2017) 116028.
[13] J.-F. Salavy, European Helium Cooled Lithium Lead (HCLL) Test BlanketModule (TBM) Detailed Description Document (DDD), CEA Report (2005) Saclay, France.
[14] V.S. Udintsev, P. Maquet, E. Alexandrov, et al., Final design of the generic equatorial port plug structure for ITER diagnostic systems, Fusion Eng. Des. 96 (2015) 993–997.
[15] J.M. Drevon, M. Walsh, P. Andrew, et al., Process and overview of diagnostics integration in ITER ports, Fusion Eng. Des. 88 (6-8) (2013) 1306–1309.
[16] M. Lei, S. Xu, C. Guo, et al., Design and thermal-hydraulic evaluation of helium-cooled ceramic breeder blanket for China fusion engineering test reactor, Int. J. Energy Res. 42 (10) (2017).
[17] M.Z. Lei, S.L. Xu, J. Wang, et al., Preliminary assessment on safety performance of updated HCCB blanket module for CFETR, Fusion Eng. Des. 131 (2018) 77–83.
[18] G. Vayakis, E.R. Hodgson, V. Voitsenya, et al., Generic diagnostic issues for a burning plasma experiment, Chapter 12, Fusion Sci. Technol. 53 (2) (2008) 699–750.
[19] M. Bakhtiari, M. Azumi, K. Tsuzuki, et al., Effect of a ferromagnetic wall on low β tearing modes in the Japan Atomic Energy Research Institute Fusion Torus-2 Modified, Phys. Plasmas 10 (8) (2003) 3212–3216.
[20] R. Albanese, R. Fresa, M.F. Palumbo, et al., Electromagnetic disruption loads on ITER blanket modules, IEEE Trans. Magn. 46 (8) (2010) 2935–2938.
[21] ANSYS 14.0 APDL manual.
[22] S. Liu, M. Chen, M. Lei, et al., Electromagnetic and structural analysis on vacuum vessel for CFETR during plasma major disruption, J. Fusion Energy 33 (6) (2014) 713–719.